

Evolution of the cosmic ray anisotropy above 10^{14} eV

M. Aglietta^{1,2}, V.V. Alekseenko³, B. Alessandro², P. Antonioli⁴, F. Arneodo⁵,
 L. Bergamasco^{2,6}, M. Bertaina^{2,6}, R. Bonino^{1,2}, A. Castellina^{1,2}, A. Chiavassa^{2,6},
 B. D’Ettorre Piazzoli⁷, G. Di Sciascio^{7,8}, W. Fulgione^{1,2}, P. Galeotti^{2,6}, P.L. Ghia^{1,5,9},
 M. Iacovacci⁷, G. Mannocchi^{1,2}, C. Morello^{1,2}, G. Navarra^{2,6}, O. Saavedra^{2,6},
 A. Stamerra^{6,10}, G.C. Trinchero^{1,2}, S. Valchierotti^{2,6}, P. Vallania^{1,2}, S. Vernetto^{1,2},
 C. Vigorito^{2,6}
 (The EAS-TOP Collaboration)

ABSTRACT

The amplitude and phase of the cosmic ray anisotropy are well established experimentally between 10^{11} eV and 10^{14} eV. The study of their evolution into the energy region $10^{14} - 10^{16}$ eV can provide a significant tool for the understanding of the steepening (“knee”) of the primary spectrum. In this letter we extend the EAS-TOP measurement performed at $E_0 \approx 10^{14}$ eV, to higher energies by using the full data set (8 years of data taking). Results derived at about 10^{14} and $4 \cdot 10^{14}$ eV are compared and discussed. Hints of increasing amplitude and change of phase above 10^{14} eV are reported. The significance of the observation for the understanding of cosmic ray propagation is discussed.

Subject headings: Cosmic rays, diffusion

1. Introduction

The steepening (“knee”) observed at $E_0 \approx 3 \cdot 10^{15}$ eV represents a main feature of the energy spectrum of cosmic rays and its characterization is therefore a main tool for the understanding of

the galactic radiation. Composition studies have shown that it is related to the steepening of the lightest primaries (protons, helium, CNO) spectra (Aglietta et al. 2004; Antoni et al. 2005).

Such effect can be due, on the one side, to energy limits of the acceleration process at the source, namely diffusive shock acceleration in supernova remnants, generally considered to be the sources of galactic cosmic rays. The maximum energy of the accelerated protons is, indeed, calculated to occur in the 10^{15} eV energy region (Berezhko et al 1996; Berezhko & Volk 2007), but could reach up to about 10^{17} eV (Ptuskin & Zirakashvili 2003). On the other side, this feature has been possibly explained in terms of a change in the cosmic ray propagation properties inside the Galaxy (Peters 1960; Zatsepin et al. 1962). Galactic propagation is described through diffusion models whose parameters have been obtained through composition studies (mainly from the ratio of secondary to primary nuclei) at energies well below 1 TeV (see e.g. (Jones et al.

¹Istituto di Fisica dello Spazio Interplanetario, INAF, Torino, Italy

²Istituto Nazionale di Fisica Nucleare, Torino, Italy

³Institute for Nuclear Research, AS Russia, Baksan Neutrino Observatory, Russia

⁴Istituto Nazionale di Fisica Nucleare, Bologna, Italy

⁵Laboratori Nazionali del Gran Sasso, INFN, Assergi (AQ), Italy

⁶Dipartimento di Fisica Generale dell’Università, Torino, Italy

⁷Dipartimento di Scienze Fisiche dell’Università and INFN, Napoli, Italy

⁸Presently at Istituto Nazionale di Fisica Nucleare, Roma Tor Vergata, Italy

⁹Presently at Institut de Physique Nucleaire, CNRS, Orsay, France

¹⁰Presently at Dipartimento di Fisica dell’Università and INFN, Pisa, Italy

2001; Strong et al. 2007)). The diffusion coefficient, D , is found to increase with magnetic rigidity ($D \propto R^{0.6}$, or $D \propto R^{0.3}$ for models including reacceleration). However, no confirmation, and no information has till now been obtained at higher energies, where the main observable is represented by the large scale anisotropy in the cosmic rays arrival directions, that is known to be strictly related to the diffusion coefficient (see e.g. (Berezinsky et al. 1990)). The study of the evolution of the anisotropy in the “knee” energy region can therefore provide a significant test of the diffusion models, and a valuable insight for the discrimination between the two possible explanations of the spectral steepening.

At $E_0 \approx 10^{14}$ eV the EAS-TOP¹ results (Aglietta et al. 1996) demonstrated that the main features of the anisotropy (i.e. of cosmic ray propagation) are similar to the ones measured at lower energies ($10^{11} \div 10^{14}$ eV), both with respect to amplitude ($(3 \div 6) \cdot 10^{-4}$) and phase ($(0 \div 4)$ h LST) (Gombosi et al. 1975; Fenton et al. 1975; Nagashima et al. 1989; Alekseenko et al. 1981; Andreev et al. 1987; Ambrosio et al. 2003; Munakata et al. 1997; Amenomori et al. 2005; Guillian et al. 2007; Abdo et al. 2008). At higher energies the limited statistics does not allow to draw any firm conclusion (Kifune et al. 1984; Gherardy et al. 1983; Antoni et al. 2004; Amenomori et al. 2006; Over et al. 2007).

In this letter we present the EAS-TOP measurement based on the full data-set and we extend the analysis to about $4 \cdot 10^{14}$ eV.

2. The experiment and the analysis

The EAS-TOP Extensive Air Shower array was located at Campo Imperatore (2005 m a.s.l., lat. $42^\circ 27'$ N, long. $13^\circ 34'$ E, INFN Gran Sasso National Laboratory). The electromagnetic detector (used for the present analysis) (Aglietta et al. 1993) consisted of 35 modules of scintillator counters, 10 m^2 each, distributed over an area of about 10^5 m^2 . The trigger was provided by the coincidence of any four neighbouring modules (threshold $n_p \approx 0.3$ m.i.p./module), the event rate being $f \approx 25$ Hz. The data under discussion have been collected between January 1992 and December 1999

¹The Extensive Air Shower array on TOP of the Gran Sasso underground laboratories.

for a total of 1431 full days of operation.

To select different primary energies, a cut is applied to the events based on the number of triggered modules (see table 1). The average primary energies are evaluated for primary protons and QGSJET01 hadron interaction model (Kalmykov et al. 1997) in CORSIKA (Heck & Knapp 1998).

Table 1: *Characteristics of the two classes of events used in the analysis: number of triggered modules, primary energy and number of collected events in the East+West sectors.*

Class	$N_{modules}$	E_0 [eV]	N_{EW}
I	≥ 4	$1.1 \cdot 10^{14}$	$1.5 \cdot 10^9$
II	≥ 12	$3.7 \cdot 10^{14}$	$1.7 \cdot 10^8$

For the analysis of the anisotropy, we adopt a method based on the counting rate differences between East-ward and West-ward directions, that allows to remove counting rate variations of atmospheric origin. The events used in the analysis (see table 1) are the ones with azimuth angle ϕ inside $\pm 45^\circ$ around the East and West directions, and zenith angle $\theta < 40^\circ$. The difference between the number of counts measured from the East sector, $C_E(t)$, and from the West one, $C_W(t)$, at time t in a fixed interval ($\Delta t = 20$ min), is related to the first derivative of the intensity $I(t)$ as: $\frac{dI}{dt} \simeq D(t) = \frac{C_E(t) - C_W(t)}{\delta t}$ where δt is the average hour angle between the vertical and each of the two sectors (1.7 h in our case). The harmonic analysis is performed on the differences $D(t)$; the amplitudes and phases of the variation of $I(t)$ are obtained through the integration of the corresponding terms of the Fourier series (Aglietta et al. 2007).

3. Results

The harmonic analysis has been performed in solar, sidereal and anti-sidereal time². We describe in sect 3.1 the results of the analysis, while

²The anti-sidereal time is a fictitious time scale symmetrical to the sidereal one with respect to the solar time and that reflects seasonal influences (Farley & Storey 1954).

$E_0[\text{eV}]$	$A_{sol}^I 10^4$	$\phi_{sol}^I [\text{h}]$	$P_{sol}^I (\%)$	$A_{sid}^I 10^4$	$\phi_{sid}^I [\text{h}]$	$P_{sid}^I (\%)$	$A_{asid}^I 10^4$	$\phi_{asid}^I [\text{h}]$	$P_{asid}^I (\%)$
$1.1 \cdot 10^{14}$	2.8 ± 0.8	6.0 ± 1.1	0.2	2.6 ± 0.8	0.4 ± 1.2	0.5	1.2 ± 0.8	23.9 ± 2.8	32.5
$3.7 \cdot 10^{14}$	3.2 ± 2.5	6.0 ± 3.4	44.1	6.4 ± 2.5	13.6 ± 1.5	3.8	3.4 ± 2.5	22.3 ± 3.2	39.7
	$A_{sol}^{II} 10^4$	$\phi_{sol}^{II} [\text{h}]$	$P_{sol}^{II} (\%)$	$A_{sid}^{II} 10^4$	$\phi_{sid}^{II} [\text{h}]$	$P_{sid}^{II} (\%)$	$A_{asid}^{II} 10^4$	$\phi_{asid}^{II} [\text{h}]$	$P_{asid}^{II} (\%)$
$1.1 \cdot 10^{14}$	1.4 ± 0.8	7.0 ± 1.2	21.6	2.3 ± 0.8	6.3 ± 0.7	1.6	0.6 ± 0.8	-	75.5
$3.7 \cdot 10^{14}$	1.7 ± 2.5	-	79.4	1.5 ± 2.5	-	83.5	1.2 ± 2.5	-	89.1

Table 2: Results of the analysis of the first (amplitude A^I , phase ϕ^I , and Rayleigh imitation probability P^I) and second harmonic (A^{II} , ϕ^{II} , P^{II}) in solar (columns 2-4), sidereal (columns 5-7), and anti-sidereal time (columns 8-10). Phases are not defined when amplitudes are smaller than their uncertainties.

in sect. 3.2 we show the related counting rate curves.

3.1. The harmonic analysis

For the two different primary energies, the reconstructed amplitudes and phases of the first and second harmonics are shown in table 2, together with the corresponding Rayleigh imitation probabilities (P).

– Concerning the **first harmonic**:

(a) At $1.1 \cdot 10^{14}$ eV, from the analysis in solar time, the obtained amplitude and phase ($A_{sol}^I = (2.8 \pm 0.8) \cdot 10^{-4}$, $\phi_{sol}^I = (6.0 \pm 1.1)$ h, $P_{sol}^I = 0.2\%$) are in excellent agreement with the expected ones from the Compton-Getting effect (Compton & Getting 1935) due to the revolution of the Earth around the Sun: at our latitude $A_{sol,CG} = 3.0 \cdot 10^{-4}$, $\phi_{sol,CG} = 6.0$ h.

With respect to the sidereal time analysis, the measured amplitude and phase ($A_{sid}^I = (2.6 \pm 0.8) \cdot 10^{-4}$, $\phi_{sid}^I = (0.4 \pm 1.2)$ h LST), with imitation probability $P_{sid}^I = 0.5\%$, confirm the previous EAS-TOP result (Aglietta et al. 1996).

Bi-monthly vectors representing the first harmonic are shown in figure 1 (dots), together with the expected ones (stars) from the measured solar and sidereal amplitudes. The expected anti-clockwise rotation of the vector is clearly visible, showing that, at any time, the composition of the two vectors is observed, and that the expected and measured individual values are fully compatible within the statistical uncertainties.

(b) At $3.7 \cdot 10^{14}$ eV the amplitude and phase of the measured first harmonic in solar time are

still consistent with the expected ones for the solar Compton-Getting effect, although, due to the reduced statistics, the chance imitation probability is rather high.

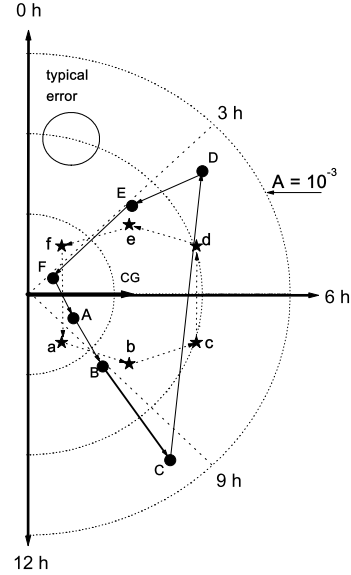


Fig. 1.— Bi-monthly solar vectors at $1.1 \cdot 10^{14}$ eV. Capital and small letters refer respectively to the expected and theoretical points ($A, a = \text{Jan} + \text{Feb}$; $B, b = \text{Mar} + \text{Apr}$; $C, c = \text{May} + \text{Jun}$; $D, d = \text{Jul} + \text{Aug}$; $E, e = \text{Sep} + \text{Oct}$; $F, f = \text{Nov} + \text{Dec}$). The typical vector statistical uncertainty is shown.

Concerning the analysis in sidereal time, we obtain $A_{sid}^I = (6.4 \pm 2.5) \cdot 10^{-4}$, $\phi_{sid}^I = (13.6 \pm 1.5)$ h LST, with an imitation probability of about 3.8%.

This indicates therefore a change of phase (from 0.4 to 13.6 h) and an increase of amplitude (by a factor 2.5) with respect to the first harmonic measured at $1.1 \cdot 10^{14}$ eV.

– Concerning the **second harmonic** most significant ($P_{sid}^{II} = 1.6\%$) is the amplitude observed in sidereal time in the lower energy class of events (comparable with the first harmonic one: $A_{sid}^{II} = (2.3 \pm 0.8) \cdot 10^{-4}$, $\phi_{sid}^{II} = (6.3 \pm 0.7)$ h LST) (see also (Aleksenko et al. 1981)).

Both at $1.1 \cdot 10^{14}$ eV and $3.7 \cdot 10^{14}$ eV, no significant amplitude is observed in anti-sidereal time, showing that no additional correction is required due to residual seasonal effects.

3.2. The counting rate curves

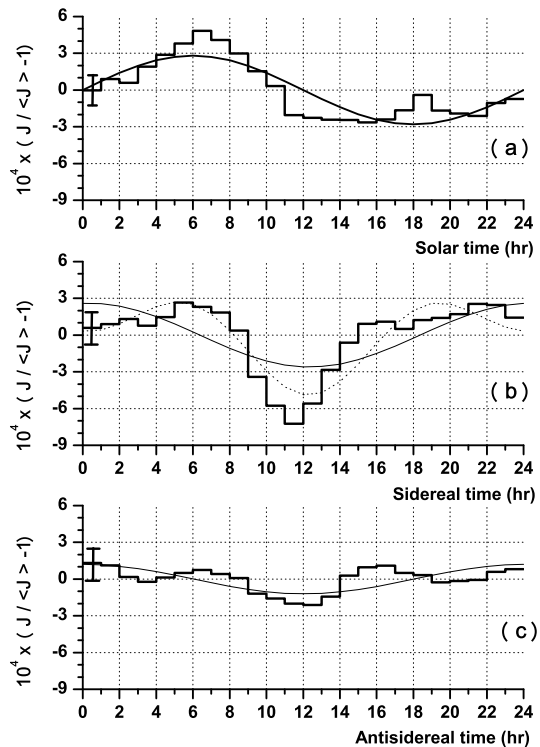


Fig. 2.— *Thick black lines: counting rate curves in solar (a), sidereal (b) and anti-sidereal (c) time at $1.1 \cdot 10^{14}$ TeV. The statistical uncertainty for each bin is given in the first one. The curves resulting from the first harmonic analysis are also shown (light black lines); for the sidereal time curve, the combination of first and second harmonic (dotted black line) is additionally superimposed.*

Besides the harmonic analysis, it is interesting to visualize the variations of the cosmic ray intensity versus time, $I(t)$, as reconstructed by integration of the East-West differences, $D(t)$. They are shown in figs. 2 and 3, for the classes of events at $1.1 \cdot 10^{14}$ eV and $3.7 \cdot 10^{14}$ eV, respectively (a,b,c for solar, sidereal, and anti-sidereal time scales).

As already shown by the harmonic analysis, at both energies the curves in solar time are dominated by the Compton-Getting effect due to the motion of the Earth, and no modulation is visible in the anti-sidereal time scale.

A main difference is observed in the sidereal time curves: while the shape of the curve at $1.1 \cdot 10^{14}$ eV is in remarkable agreement with the EAS and muon measurements reported at and below 100 TeV, the curve related to the highest energy class of events is characterized by a broad excess around 13-16 h LST.

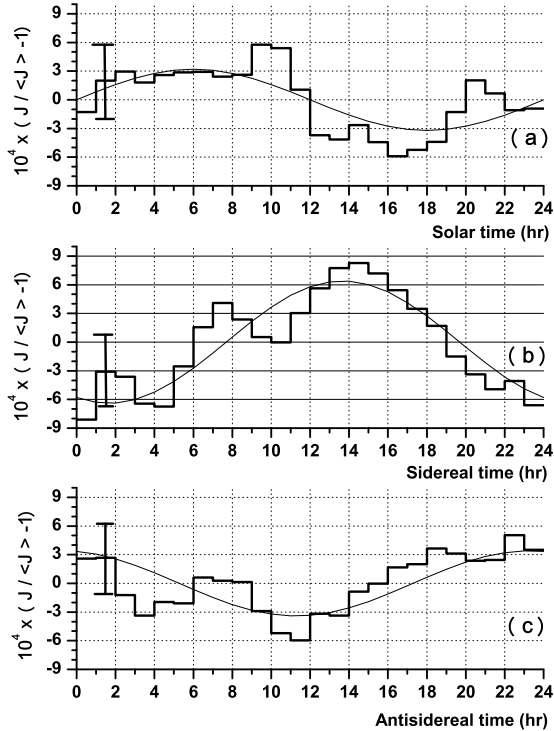


Fig. 3.— *Thick black lines: counting rate curves in solar (a), sidereal (b) and anti-sidereal (c) time at $3.7 \cdot 10^{14}$ TeV. The curves resulting from the first harmonic analysis are also shown (light black lines).*

4. Conclusions

High stability data obtained from long time observations (8 years) from the EAS-TOP array confirm the amplitude and phase of the cosmic ray anisotropy already reported at 10^{14} eV: $A_{sid}^I = (2.6 \pm 0.8) \cdot 10^{-4}$, $\phi_{sid}^I = (0.4 \pm 1.2)$ h LST, with Rayleigh imitation probability $P_{sid}^I = 0.5\%$. The result is supported by the observation of the Compton-Getting effect due to the revolution of the Earth around the Sun, and by the absence of

anti-sidereal effects. It confirms the homogeneity of the anisotropy data over the energy range 10^{11} - 10^{14} eV.

At higher energies (around $4 \cdot 10^{14}$ eV) the observed anisotropy shows a larger amplitude, $A_{sid}^I = (6.4 \pm 2.5) \cdot 10^{-4}$, and a different phase, $\phi_{sid}^I = (13.6 \pm 1.5)$ h LST, with an imitation probability of 3.8%. The statistical significance is still limited, but the measurement has the highest sensitivity with respect to previous experiments at these energies, and it is not in contradiction with any of them.

The dependence of the anisotropy amplitude over primary energy ($A \propto E_0^\delta$) deduced from the present two measurements can be represented by a value of $\delta = 0.74 \pm 0.41$. Therefore, at least in the energy range $(1-4) \cdot 10^{14}$ eV, such dependence is compatible with that of the diffusion coefficient as derived by composition measurements at lower energies.

On another side, the sharp increase of the anisotropy above 10^{14} eV may be indicative of a sharp evolution of the propagation properties, and therefore of the diffusion coefficient just approaching the steepening of the primary spectrum. This opens the problems of obtaining an improved theoretical and experimental description of the whole evolution of the diffusion processes vs primary energy, and understanding how such evolution could affect the energy spectra at the "knee". From the experimental point of view, the extension of the anisotropy measurements with high sensitivity to and above 10^{15} eV will be of crucial significance.

V.V.A. is grateful to the INFN Gran Sasso National Laboratory for financial support through FAI funds. P.L.G. acknowledges the financial support by the European Community 7th Framework Program through the Marie Curie Grant PIEF-GA-2008-220240.

REFERENCES

- Aglietta, M. et al. 2004, *Astrop. Phys.*, 21, 583
- Antoni, T. et al. 2005, *Astrop. Phys.*, 24, 1
- Ptuskin, V.S., & Zirakashvili, V.N. 2003, *A&A*, 403, 1
- Berezhko, E.G. et al. 1996, *JETP*, 82, 1

- Berezhko, E.G., & Volk, H.J. 2007, ApJ, 661, L175
- Peters, P. 1960, Proc. 6th ICRC, Vol. 3, 157
- Zatsepin, G.T. et al. 1962, Izv. Akad. Nauk USSR S.P., 26, 685
- Jones, F.C. et al. 2001, ApJ, 547, 264
- Strong, A.W et al, 2007, Annual Review of Nuclear and Particle Science, 50, 1, 285
- Berezinsky, V. et al. 1990, Astrophysics of Cosmic Rays, North Holland (V.L. Ginzburg ed.)
- Aglietta, M. et al. 1996, ApJ, 470, 501
- Gombosi, T. et al. 1975, Nature, 255, 687
- Fenton, B.K. et al. 1975, Proc. 14th ICRC, 4, 1482
- Nagashima, K. et al. 1989, Il Nuovo Cimento C, 12, 695
- Alekseenko, V.V. et al. 1981, Proc. 17th ICRC, 1, 146
- Andreev, Y. et al. 1987, Proc. 20th ICRC, 2, 22
- Ambrosio, M. et al. 2003, Phys. Rev. D, 67, 042002
- Munakata, K. et al 1997, Phys. Rev. D, 56, 23
- Amenomori, M. et al. 2005, ApJ, 626, L29
- Guillian, G. et al. 2007, Phys. Rev. D, 75, 062003
- Abdo, A. A. et al. 2008, arXiv:0806.2293
- Kifune, T. et al. 1984, J. Phys. G, 12, 129
- Gherardy, P. et al. 1983, J. Phys. G, 9, 1279
- Antoni, T. et al. 2004, Ap. J., 604, 687
- Amenomori, M. et al. 2006, Science, 314, 439
- Over, S. et al. 2007, Proc. 30th ICRC
- Aglietta, M. et al. 1993, Nucl. Instr. Meth. Phys. Res. A., 336, 310
- Kalmykov, N. N. et al. 1997, Nucl. Phys. B, 52B, 17
- Heck, D. et al. 1998, FZK Report, 6019
- Aglietta, M. et al. 2007, Proc. 30th ICRC
- Farley, F. J. M., & Storey, J. R. et al. 1954, Proc. Phys. Soc., 67, 996
- Compton, A.H., & Getting, I. A. 1935, Phys. Rev, 47, 817

This 2-column preprint was prepared with the AAS L^AT_EX macros v5.2.